



## Reduction of free-edge stress intensities in anisotropic bimetals

J.R. BERGER<sup>1</sup>, P.A. MARTIN<sup>2</sup> and J.P. LIEN<sup>1</sup>

<sup>1</sup>*Division of Engineering, Colorado School of Mines, Golden, Colorado, U.S.A. e-mail: jberger@mines.edu*

<sup>2</sup>*Department of Mathematics, University of Manchester, Manchester M13 9PL, U.K.*

Received 12 November 1997; accepted in revised form 3 June 1998

**Abstract.** We investigate the free-edge stresses in anisotropic bimetals through the use of the free-edge stress intensity factor,  $K_f$ . This requires a determination of the singularity order at the free-surface as well as a calculation of the near-field stresses. We determine the order of the singularity for arbitrary free-surface orientation of the upper material using an eigenvalue analysis for anisotropic bimetals. The interfacial stresses are determined using a boundary element calculation based on anisotropic, bimaterial Green's functions. The variation of  $K_f$  with free-surface orientation is determined. We find that the free-edge singularity vanishes for certain angles dependent on the anisotropic elastic constants.

**Key words:** Anisotropic elasticity, boundary element analysis, free-edge stress intensity, Green's functions.

### 1. Introduction

Layered materials are subject to failure initiation where an interface meets a free surface in the composite solid. The initiation of failure at these sites can be interpreted mathematically by the stress singularity at such a location. The nature of the singularity has been investigated by many researchers including Zwiers, Ting and Spilker (1982), Ting (1996), Bogy (1972), Dundurs (1969), Hein and Erdogan (1971), Bak and Koenig (1994), Ding and Kumosa (1994), Tewary (1991), Tewary and Kriz (1991) and Reedy (1990). These investigations were primarily concerned with composite solids whose free surfaces were oriented at either  $\pm 90^\circ$  or at an arbitrary symmetric angle with respect to the interface. In this paper, we investigate singular stresses in anisotropic bimetals where the interface intersects the free surface and the angle of the upper material with respect to the interface is varied. The free surface orientation of the material below the interface is maintained at  $90^\circ$ . The geometry of the general problem is shown in Figure 1.

In general, there are two calculations involved with assessing the intensity of stress at the intersection of the interface with the free surface. The near-field stresses at such a point are singular,

$$\sigma_{ij}(r, \theta) \approx K_f r^\delta \Sigma_{ij}(\theta), \quad (1)$$

where  $r, \theta$  are polar coordinates situated at the intersection with the free surface and  $\delta$  is the order of the singularity ( $\text{Re } \delta < 0$ ). Following Reedy (1990), the free-surface stress intensity factor  $K_f$  can be defined as

$$K_f = \lim_{r \rightarrow 0} \{\sigma_{22}(r, 0)r^{-\delta}\}, \quad (2)$$

where  $x_2 = 0$  and  $\theta = 0$  is the interface. To investigate the stress intensity at the free surface therefore requires two calculations. First, we must determine the order of the singularity  $\delta$  for

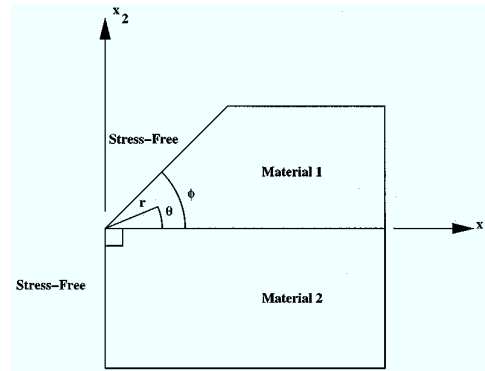


Figure 1. Anisotropic bimaterial with arbitrary free-surface orientation of the upper material.

the particular material system and free-surface orientation of interest. Second, the stresses on the interface near the free surface must be accurately calculated in order to obtain  $K_f$  from (2).

In this paper we first review the procedure of Ting (1996) for the determination of the order of the singularity  $\delta$  in anisotropic bimaterials. We next investigate the singularity order for a variety of free-surface angles. With reference to Figure 1, of special interest are those angles  $\phi$  for which the singularity order is zero. From a practical viewpoint, this indicates a nonsingular state of stress where delamination initiation at the free edge is suppressed. Theoretically, this implies that (1) is incomplete at such special angles; a weak logarithmic singularity may still be present (Ting, 1996, Section 9.6).

We next describe the determination of the state of stress on the interface through a boundary element calculation where the kernels of the boundary integrals are Green's functions for anisotropic bimaterials. The use of these particular Green's functions allow us to only discretize the remote boundary of the specimen. All interfacial boundary conditions are satisfied with the Green's function so no interface discretization is necessary. Finally, we provide some example calculations for the free-edge stress intensity factor as a function of free-surface orientation angles  $\phi$  for copper-silicon, nickel-copper, and solder-copper bimaterial systems.

## 2. Determination of the singularity order $\delta$

The order of the singularity at a free edge in an anisotropic bimaterial problem may either be determined through the eigenvalue analysis of Zwiers, Ting and Spilker (1982) and Ting (1996) or with a Green's function technique used by Tewary (1991) and Tewary and Kriz (1991). For this investigation, we selected the eigenvalue approach since we were investigating problems with a variable angle of the upper free surface  $\phi$ . The Green's function method as developed in Tewary (1991) is specifically for the case of  $\phi = 90^\circ$ . The Green's function technique has the distinct advantage over the eigenvalue approach of not requiring the determination of complex roots of a high-order, complex polynomial. However, there is added complexity with the Green's function approach due to the necessity of solving a Hilbert problem. For the problem under consideration here, the eigenvalue approach provides a direct method for determining the singularity order  $\delta$ .

The eigenvalue analysis for the singularity order  $\delta$  is based on the technique of Stroh (1958). Following Ting (1996, Section 9.6), the displacements and stress function in an anisotropic bimaterial can be written as

$$\mathbf{u}^{(n)} = r^{\delta+1} \{ \mathbf{A}^{(n)} \langle \zeta^{(n)\delta+1}(\theta) \rangle \mathbf{q}^{(n)} + \overline{\mathbf{A}}^{(n)} \langle \overline{\zeta}^{(n)\delta+1}(\theta) \rangle \tilde{\mathbf{q}}^{(n)} \}, \quad (3)$$

$$\mathbf{F}^{(n)} = r^{\delta+1} \{ \mathbf{B}^{(n)} \langle \zeta^{(n)\delta+1}(\theta) \rangle \mathbf{q}^{(n)} + \overline{\mathbf{B}}^{(n)} \langle \overline{\zeta}^{(n)\delta+1}(\theta) \rangle \tilde{\mathbf{q}}^{(n)} \}, \quad (4)$$

where the superscript  $n = 1, 2$  indicates either the upper or lower material,  $\mathbf{A}$  and  $\mathbf{B}$  are  $3 \times 3$  complex matrices,  $\mathbf{q}$  and  $\tilde{\mathbf{q}}$  are  $3 \times 1$  complex vectors, the angled brackets denote a diagonal matrix, and an overbar indicates a complex conjugate. If  $\delta$  is real,  $\tilde{\mathbf{q}}$  is the complex conjugate of  $\mathbf{q}$ . If  $\delta$  is complex,  $\tilde{\mathbf{q}}$  is not necessarily the complex conjugate of  $\mathbf{q}$ . The elements of the diagonal matrices appearing in (3)–(4) are

$$\langle \zeta(\theta) \rangle_\alpha = \zeta_\alpha(\theta); \quad \alpha = 1, 2, 3, \quad (5)$$

where we have omitted the superscript  $n$  for clarity. The complex variable  $\zeta_\alpha$  is defined through the polar form of the variable  $z_\alpha$  as

$$z_\alpha = r(\cos \theta + p_\alpha \sin \theta) = r\zeta_\alpha(\theta), \quad (6)$$

where

$$z_\alpha = x_1 + p_\alpha x_2. \quad (7)$$

The determinant  $|\mathbf{D}|$  needed for calculating the roots  $p_\alpha$  can be conveniently written in the form used by Ting (1996)

$$|\mathbf{D}| = |\mathbf{Q} + p(\mathbf{R} + \mathbf{R}^T) + p^2\mathbf{T}| = 0, \quad (8)$$

where the  $3 \times 3$  matrices  $\mathbf{Q}$ ,  $\mathbf{R}$ , and  $\mathbf{T}$  are, in terms of the anisotropic elastic constants,

$$Q_{ik} = c_{i1k1}, \quad R_{ik} = c_{i1k2}, \quad T_{ik} = c_{i2k2}. \quad (9)$$

The roots  $p_\alpha$  of the sextic equation, (8), occur in complex conjugate pairs. The remaining terms appearing in (3) and (4) are defined with the right eigenvalues  $\mathbf{a}$ ,

$$\mathbf{D}\mathbf{a} = \{ \mathbf{Q} + p(\mathbf{R} + \mathbf{R}^T) + p^2\mathbf{T} \} \mathbf{a} = 0, \quad (10)$$

$$\mathbf{b} = (\mathbf{R}^T + p\mathbf{T})\mathbf{a}. \quad (11)$$

The matrices  $\mathbf{A}$  and  $\mathbf{B}$  in (3) and (4) are then

$$\mathbf{A}^{(n)} = [\mathbf{a}_1^{(n)} \quad \mathbf{a}_2^{(n)} \quad \mathbf{a}_3^{(n)}], \quad (12)$$

$$\mathbf{B}^{(n)} = [\mathbf{b}_1^{(n)} \quad \mathbf{b}_2^{(n)} \quad \mathbf{b}_3^{(n)}]. \quad (13)$$

The components of the stress function in (4) are related to the Cartesian stress components as

$$\sigma_{i1} = -F_{i,2}, \quad \sigma_{i2} = F_{i,1}. \quad (14)$$

Equations (3) and (4) can be written for continuity of displacement and traction across the bimaterial interface and at the traction-free surfaces shown in Figure 1,  $(r, \theta) = (r, -\frac{1}{2}\pi)$  and  $(r, \theta) = (r, \phi)$ . This yields a set of 12 equations which can be solved for the singularity order  $\delta$ . However, a more efficient solution can be obtained by using the orthogonality and closure relations (Mantic and Paris, 1996; Ting, 1996) which relate the matrices  $\mathbf{A}$  and  $\mathbf{B}$  as

$$\mathbf{B}^T \mathbf{A} + \mathbf{A}^T \mathbf{B} = \overline{\mathbf{B}}^T \overline{\mathbf{A}} + \overline{\mathbf{A}}^T \overline{\mathbf{B}} = \mathbf{I}, \quad (15)$$

$$\mathbf{B}^T \overline{\mathbf{A}} + \mathbf{A}^T \overline{\mathbf{B}} = \overline{\mathbf{B}}^T \overline{\mathbf{A}} + \overline{\mathbf{A}}^T \overline{\mathbf{B}} = \mathbf{0}, \quad (16)$$

$$\mathbf{A} \mathbf{B}^T + \overline{\mathbf{A}} \overline{\mathbf{B}}^T = \mathbf{B} \mathbf{A}^T + \overline{\mathbf{B}} \overline{\mathbf{A}}^T = \mathbf{I}, \quad (17)$$

$$\mathbf{A} \mathbf{A}^T + \overline{\mathbf{A}} \overline{\mathbf{A}}^T = \mathbf{B} \mathbf{B}^T + \overline{\mathbf{B}} \overline{\mathbf{B}}^T = \mathbf{0}. \quad (18)$$

The vectors  $\mathbf{a}$  and  $\mathbf{b}$  must be properly normalized (Ting, 1996) for these relations to hold. Equations (3) and (4) written for continuity of traction and displacement across the interface are then

$$\mathbf{A}^{(1)} \mathbf{q}_1 + \overline{\mathbf{A}}^{(1)} \tilde{\mathbf{q}}_1 = \mathbf{A}^{(2)} \mathbf{q}_2 + \overline{\mathbf{A}}^{(2)} \tilde{\mathbf{q}}_2 = \mathbf{h}, \quad (19)$$

$$\mathbf{B}^{(1)} \mathbf{q}_1 + \overline{\mathbf{B}}^{(1)} \tilde{\mathbf{q}}_1 = \mathbf{B}^{(2)} \mathbf{q}_2 + \overline{\mathbf{B}}^{(2)} \tilde{\mathbf{q}}_2 = \mathbf{g}, \quad (20)$$

using the fact that  $\zeta_\alpha^{(n)}(0) = 1$  by our choice of coordinate system. The boundary condition at the traction-free surface at  $\theta = \phi$  is then (cf. Ting, 1996, Equation (9.6-6))

$$\begin{aligned} & [\mathbf{B}^{(1)} \langle \zeta^{(1)d+1}(\phi) \rangle \mathbf{B}^{(1)T} + \overline{\mathbf{B}}^{(1)} \langle \zeta^{(1)d+1}(\phi) \rangle \overline{\mathbf{B}}^{(1)T}] \mathbf{h} \\ & + [\mathbf{B}^{(1)} \langle \zeta^{(1)\delta+1}(\phi) \rangle \mathbf{A}^{(1)T} + \overline{\mathbf{B}}^{(1)} \langle \zeta^{(1)\delta+1}(\phi) \rangle \overline{\mathbf{A}}^{(1)T}] \mathbf{g} = \mathbf{0}. \end{aligned} \quad (21)$$

The boundary condition at the traction-free surface at  $\theta = -\pi/2$  is

$$\begin{aligned} & [\mathbf{B}^{(2)} \langle \zeta^{(2)\delta+1}(-\frac{1}{2}\pi) \rangle \mathbf{B}^{(2)T} + \overline{\mathbf{B}}^{(2)} \langle \zeta^{(2)\delta+1}(-\frac{1}{2}\pi) \rangle \overline{\mathbf{B}}^{(2)T}] \mathbf{h} \\ & + [\mathbf{B}^{(2)} \langle \zeta^{(2)\delta+1}(-\frac{1}{2}\pi) \rangle \mathbf{A}^{(2)T} + \overline{\mathbf{B}}^{(2)} \langle \zeta^{(2)\delta+1}(-\frac{1}{2}\pi) \rangle \overline{\mathbf{A}}^{(2)T}] \mathbf{g} = \mathbf{0}. \end{aligned} \quad (22)$$

In matrix form, (21) and (22) can be written as

$$\mathbf{M}(\delta) \begin{Bmatrix} \mathbf{h} \\ \mathbf{g} \end{Bmatrix} = \mathbf{0}, \quad (23)$$

where the matrix  $\mathbf{M}$  is formed through the coefficients appearing in (21) and (22). For a nontrivial solution, we require the determinant of the  $6 \times 6$  matrix  $\mathbf{M}$  to vanish,

$$|\mathbf{M}(\delta)| = 0. \quad (24)$$

Equation (24) is a 6th order equation whose roots are the singularity order  $\delta$ . In general, the roots of (24) may be real or complex. For the problem under consideration here we are concerned with stress singularities with bounded strain energy, so  $-1 < \text{Re}(\delta) < 0$ . Roots

Table 1. Elastic constants for the materials studied (GPa)

	$c_{11}$	$c_{12}$	$c_{44}$	H
Solder	130.8	107.0	11.9	0.0
Copper	168.4	121.4	75.4	103.8
Nickel	246.5	147.3	124.7	150.2
Silicon	165.7	63.9	79.6	57.4

with imaginary parts give rise to oscillatory singularities commonly associated with interface crack problems. For most common material systems, the imaginary parts of the roots of (24) are very small in comparison to the real parts of the roots (Tewary, 1991a). Therefore, our goal is to find the roots of (24) with  $-1 < \text{Re}(\delta) < 0$  as a function of the orientation of the free surface in the upper material for several bimaterial systems.

### 3. Singularities in cubic bimetals

We now solve (24) numerically for the singularity order  $\delta$  for three bimaterial systems whose components have cubic material symmetry. For each of the material systems investigated we will determine the variation of the singularity order with the free surface orientation of the upper material. The geometry of the material system under consideration is shown in Figure 1. The elastic constants of the anisotropic crystals considered here are given in Hirth and Lothe (1982) and summarized in Table 1. The elastic constants of solder will be specified so that the material is nearly isotropic. The isotropic elastic constants for high tin-content solder are taken from Berger (1994) and converted to the equivalent cubic elastic constants shown in Table 1. Also given in the table is the anisotropy factor  $H$  from Hirth and Lothe (1982) which is defined as

$$H = 2c_{44} + c_{12} - c_{11}, \quad (25)$$

where the contracted notation for anisotropic stiffnesses has been used (Ting, 1996; Hirth and Lothe, 1982). The anisotropy factor provides a measure of the strength of the anisotropy in cubic materials.

Equation (24) was solved numerically with a secant method for a variety of free-edge orientation angles  $\phi$  for nickel-copper, solder-copper, and copper-silicon bimetals. Because of the complications involved with finding the complex roots of (24), contour plots were first generated for the magnitude of the determinant as a function of the real and imaginary parts of the root  $\delta$ . Such plots are helpful in finding complex roots with iterative numerical schemes since the initial estimates for the real and imaginary parts of the roots may easily be obtained. A contour plot for the copper-silicon bimaterial is shown in Figure 2 for the case  $\phi = 170^\circ$ . As indicated in the figure, for this particular orientation the roots are approximately at  $\text{Re}(\delta) \approx -0.45, -0.2, -0.1$ . Note that  $\text{Im}(\delta) = 0$  for these roots. For comparison, the contour plot of the determinant for  $\phi = 100^\circ$  in the same bimaterial system is shown in Figure 3. Note in the figure that the only root with  $-1 < \text{Re}(\delta) < 0$  is very close to  $\text{Re}(\delta) = 0$ . This indicates the expected result that the order of the singularity is decreasing as the free-surface orientation

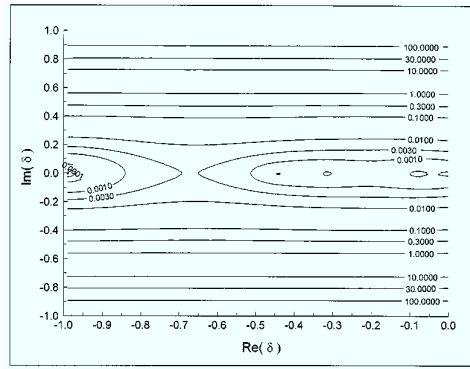


Figure 2. Contour plot of  $|\mathbf{M}(\delta)|$  vs. the real and imaginary parts of the root,  $\delta$  for  $\phi = 170^\circ$  in copper-silicon.

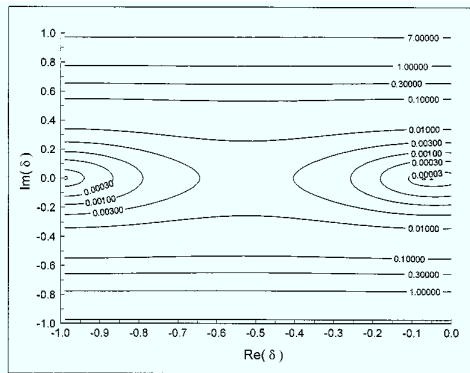


Figure 3. Contour plot of  $|\mathbf{M}(\delta)|$  vs. the real and imaginary parts of the root,  $\delta$  for  $\phi = 100^\circ$  in copper-silicon.

angle  $\phi$  is decreased. Similar results were obtained for the nickel-copper and solder-copper bimetals.

A summary plot of the magnitude of the determinant as the free-edge orientation angle  $\phi$  was varied in the copper-silicon, nickel-copper and solder-copper bimetals is shown in Figures 4–6. The maximum singularity order occurs at  $\phi = 180^\circ$  as expected. As the free-

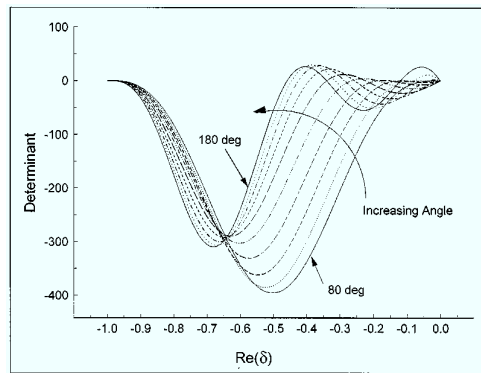


Figure 4. Plot of  $|\mathbf{M}(\delta)|$  vs. the real part of the root,  $\delta$  for several orientations  $\phi$  in copper-silicon.

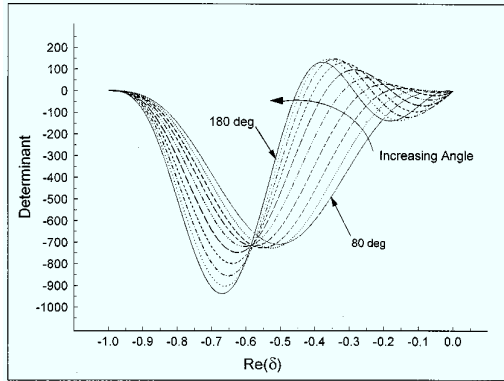


Figure 5. Plot of  $|\mathbf{M}(\delta)|$  vs. the real part of the root,  $\delta$  for several orientations  $\phi$  in nickel-copper.

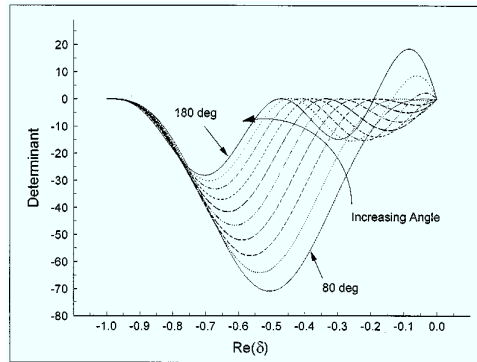


Figure 6. Plot of  $|\mathbf{M}(\delta)|$  vs. the real part of the root,  $\delta$  for several orientations  $\phi$  in solder-copper.

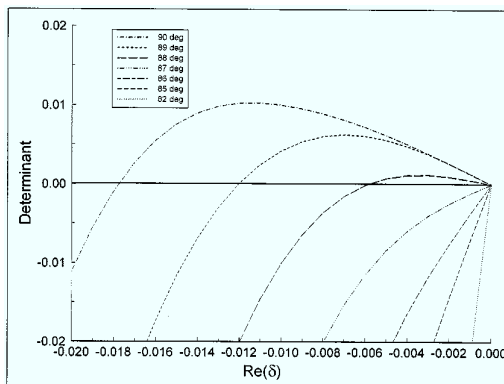


Figure 7. Finer scale plot of  $|\mathbf{M}(\delta)|$  vs. the real part of the root,  $\delta$  for  $82^\circ < \phi < 90^\circ$  in copper-silicon.

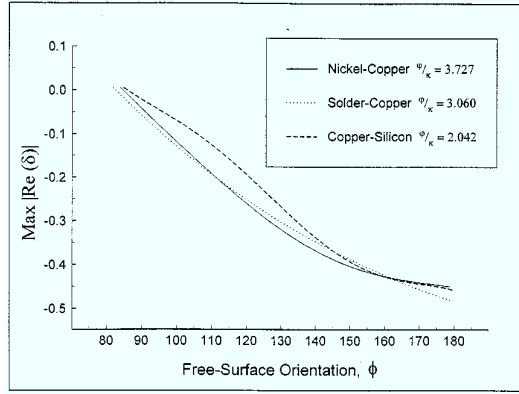


Figure 8. The order of the free-edge singularity,  $\delta$ , vs. free-surface orientation,  $\phi$  in copper-silicon, nickel-copper, and solder-copper bimaterials.

surface orientation angle  $\phi$  is reduced the singularity order moves smoothly towards zero. There is evidence in Figures 4–6 that the negative root disappears entirely somewhere for  $\phi < 90^\circ$  in each of the bimaterials. A finer-scale version of Figure 4 is shown in Figure 7 for the magnitude of the determinant in copper-silicon as  $\phi$  is varied from  $90^\circ$  to  $82^\circ$ . From Figure 7 we see that the singularity disappears for free-edge orientation angles in copper-silicon of  $\phi < 88^\circ$ . For the nickel-copper bimaterial, we find that the singularity is eliminated if  $\phi < 85^\circ$  and for the solder-copper bimaterial, we find that  $\phi < 82^\circ$  for elimination of the singularity. A summary plot of the variation of the singularity as a function of the orientation of the free-surface for each bimaterial is shown in Figure 8. Note in the figure the smooth behavior of the order of the singularity as  $\phi$  is relaxed. We have plotted the most negative  $\text{Re}(\delta)$  in  $-1 < \text{Re}(\delta) < 0$  for those cases which have multiple roots in this range.

As evident from the analysis, the critical angle below which the stress state is nonsingular is dependent on the elastic constants of the bimaterial. This can be illustrated with the generalized Dundurs constants (Ting, 1995)  $\varphi$ ,  $\kappa$  for each of the bimaterials,

$$\varphi = \frac{\nu^{(1)} - \nu^{(2)}}{\nu^{(1)} + \nu^{(2)}}, \quad (26)$$

$$\kappa = \frac{\omega^{(1)} - \omega^{(2)}}{\nu^{(1)} + \nu^{(2)}}, \quad (27)$$

where

$$\nu^{(n)} = -\frac{1}{2}(p_1^{(n)} - \bar{p}_2^{(n)})(p_2^{(n)} - \bar{p}_1^{(n)})s'_{11}, \quad (28)$$

$$\omega^{(n)} = s'_{12} - s'_{11}[\text{Re}(p_1^{(n)} p_2^{(n)})] \quad (29)$$

and  $s'_{ij}$  are the reduced elastic compliances. For the bimaterial systems studied here, the generalized Dundurs constants are given in Table 2. Shown in Figure 9 is the maximum upper free surface orientation angle for a nonsingular stress state as a function of the ratio of generalized Dundurs constants for each of the bimaterials studied here. The dependence on elastic constants of this angle is clearly indicated in the figure, although it could be argued

Table 2. Generalized dundurs constants for the bimaterial systems

Bimaterial	$\varphi$	$\kappa$	$\varphi/\kappa$
Copper-Silicon	0.323	0.158	2.042
Nickel-Copper	-0.342	-0.092	3.727
Solder-Copper	-0.731	-0.239	3.060

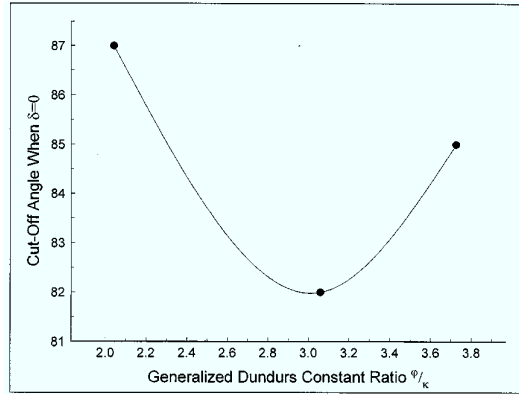


Figure 9. Maximum upper free surface orientation angle for nonsingular stresses vs. the ratio of generalized Dundurs constants.

that the dependence is weak as the variation in this angle only ranges from  $82^\circ$  to  $87^\circ$  for the bimetals studied here.

The singularity order data presented in Figure 8 is smooth so a polynomial can be fitted to the data in a least square sense. A fifth-order polynomial provided a good fit to the data over the range of  $\phi$  considered here. For free-surface orientation angles  $80^\circ < \phi < 180^\circ$  the polynomial has the form

$$\text{Re}(\delta) = \sum_{k=0}^5 C_k \phi^k. \quad (30)$$

The coefficients  $C_k$  for each of the bimetals are given in Table 3. These coefficients yield correlation coefficients of  $r = 0.99977$ ,  $0.99983$ , and  $0.99986$  for the copper-silicon, nickel-copper, and copper-solder bimetals, respectively. For any given free-edge orientation angle  $\phi$  we can therefore obtain the corresponding singularity order from (30).

#### 4. Boundary element analysis for anisotropic bimetals

Special Green's functions for anisotropic bimetals provide an ideal tool for accurately calculating the stress distribution near a bimaterial interface. Here, we use the boundary element formulation of Berger (1994) which is based on the anisotropic, bimaterial Green's function of Tewary, Wagoner, and Hirth (1989). The boundary element formulation allows us to ana-

Table 3. Polynomial coefficients for the bimetals

Bimaterial	$C_0$	$C_1$ ( $\times 10^{-2}$ )	$C_2$ ( $\times 10^{-4}$ )	$C_3$ ( $\times 10^{-6}$ )	$C_4$ ( $\times 10^{-8}$ )	$C_5$ ( $\times 10^{-11}$ )
Copper-Silicon	11.396	-47.472	78.556	-63.917	25.238	-38.683
Nickel-Copper	1.5777	-5.2001	8.4746	-8.009	3.6726	-6.3361
Copper-Solder	-1.0717	6.5702	-1.2266	9.8416	-3.6752	5.6269

lyze the general anisotropic bimaterial shown in Figure 1 where we vary  $\phi$ . The anisotropic, bimaterial Green's function is of the *general* form

$$\mathbf{U}(z_\alpha, \rho_\alpha) = \sum_\alpha \mathbf{A}(p_\alpha) \ln(z_\alpha - \rho_\alpha) + \sum_{\alpha\beta} \mathbf{B}(p_\alpha) \ln(z_\alpha - \rho_\beta), \quad (31)$$

where  $z_m$  and  $\rho_n$  are coordinates of the source and field points expressed as complex variables,  $\mathbf{A}$  and  $\mathbf{B}$  are matrices which depends on the anisotropic elastic constants and the roots of (8). The Green's function contains both free-space, singular terms as well as region-dependent, regular terms which satisfy the interfacial boundary conditions. We note that there are in fact four parts to the Green's function depending on the relative position of the source and field points with respect to the interface. The full details of the displacement and traction Green's functions for anisotropic bimetals can be found in Berger (1994).

In Berger (1994) the Green's function of (31) was used in a boundary integral formulation to analyze anisotropic bimetals. It was also shown that the Green's function degenerated to a homogeneous, anisotropic fundamental solution as well as a homogeneous, isotropic solution (the Kelvin solution) provided one was careful in dealing with the degenerate case of isotropic material behavior. The Green's function of (31) therefore represents a very general fundamental solution which can be applied to a wide variety of materials and problems in two dimensions.

The discretized boundary integral equation used in Berger (1994) with this particular Green's function is of the form

$$c_{kl} u_l(z_\alpha^m) = \sum_{j=1}^J t_i(z_\alpha^j) \frac{1}{B_\alpha^j} \int_{z_1^j}^{z_2^j} U_{ik}(z_\alpha^j, \rho_\alpha^m) dz_\alpha - \sum_{j=1}^J u_i(z_\alpha^j) \frac{1}{B_\alpha^j} \int_{z_1^j}^{z_2^j} T_{ik}(z_\alpha^j, \rho_\alpha^m) dz_\alpha, \quad (32)$$

where only the remote boundary of the solid is discretized. The interface between the two materials does not require discretization since the conditions of traction and displacement continuity are satisfied exactly by the Green's function. The integration over the remote boundary of the bimaterial is performed in the complex  $z_\alpha$ -plane using the mapping of Cruse (1988),

$$B_\alpha^j = n_1^j p_\alpha - n_2^j, \quad (33)$$

which maps a differential boundary segment to the complex  $z_\alpha$ -plane. In (33),  $n_1^j$  and  $n_2^j$  are components of the local normal vector at the  $j$ th integration element,  $p_\alpha$  is the root of (8),

and  $z_1^j, z_2^j$  are the endpoints in the complex plane of the  $j$ th integration element. In (32), the multiplier  $c_{kl}$  is  $\delta_{kl}$  for internal computation points and  $0.5\delta_{kl}$  for boundary points, and the kernels  $T_{ik}$  and  $U_{ik}$  are the traction and displacement Green's functions, respectively. Further details concerning the implementation of (32) for stress analysis is given in Berger (1994).

The specimen illustrated in Figure 1 was discretized into 96 boundary elements. The upper horizontal surface of the specimen was subjected to a uniform displacement  $u_2 = 1.0$ , and the traction  $t_1 = 0$ . The lower horizontal surface was fixed against displacement in both coordinate directions and the remaining surfaces were prescribed as stress free. For each of the bimetals studied here, the boundary element analysis was performed for free-surface orientation angles of  $\phi = 70^\circ$ – $120^\circ$  in  $10^\circ$  increments. For all bimetals and all free-surface orientation angles the same boundary conditions were imposed.

## 5. Free-edge stress intensities

We now determine the free-edge stress intensity factor  $K_f$  as defined by (2). The order of the singularity can be calculated from (30) for the free-surface orientation angles of  $\phi = 70^\circ$ – $120^\circ$  in each of the bimaterial systems. We determine the free-edge stress intensity factor by performing a least-squares collocation on  $K_f$  from (1). To perform the collocation, we use the  $\sigma_{22}$  component of stress along the interface determined from the boundary element analysis. As can be shown from a development of the eigenfunctions for  $\Sigma_{ij}(\theta)$  in (1),  $\Sigma_{22}(0) = 1$ . The  $\sigma_{22}$  stress acting on the interface in the near-field of the free edge is then given by (1) as  $\sigma_{22}(r, 0) = K_f r^\delta$ . The free-edge stress intensity factor is then calculated by a least-squares collocation of the  $\sigma_{22}$  data from the boundary element analysis as

$$K_f = \frac{\sum_{k=1}^N r_k^\delta \sigma_k}{\sum_{k=1}^N (r_k^\delta)^2}, \quad (34)$$

where  $\sigma_k = \sigma_{22}(r_k)$ . The critical assumption being made here is that the stresses used for the collocation are in the near field where the asymptotic stress given by (1) is valid. For the material systems and geometries studied here, the authors are unaware of any detailed studies of the extent of the singularity-dominated zone for the stresses given by (1). For guidance, singularity dominated zone sizes from studies of crack-tip fields in chevron-notched specimens were used from Sanford and Chona (1984). In these studies, the singular asymptotic expressions for stresses were found to be valid in the region  $r/W < 0.5$  where  $W$  is the width of the chevron-notched specimen. The data used in the collocation by (34) for the bimaterial specimens was obtained in the region  $0.04 < r/W < 0.09$  where  $W$  is the width of the specimen shown in Figure 1. This is well within the size of the singularity-dominated zone for crack-tip fields in chevron-notched specimens; future research will focus on a more exact determination of the singularity-dominated zone in materials and specimens similar to those studied here.

The collocation for  $K_f$  was performed with (34) using 10–20 data points distributed evenly along the interface with  $0.04 < r_k/W < 0.09$ . We obtain the results for free-edge stress intensity factors shown in Figure 10. We see the expected increase in  $K_f$  as the free surface orientation angle is increased. Note that  $K_f$  is simply the local value of  $\sigma_{yy}$  for the case  $\phi = 70^\circ$  since  $\delta = 0$  for this particular angle. The stress intensity is approaching an asymptotic limit for each bimaterial system under the particular loading studied here since we are

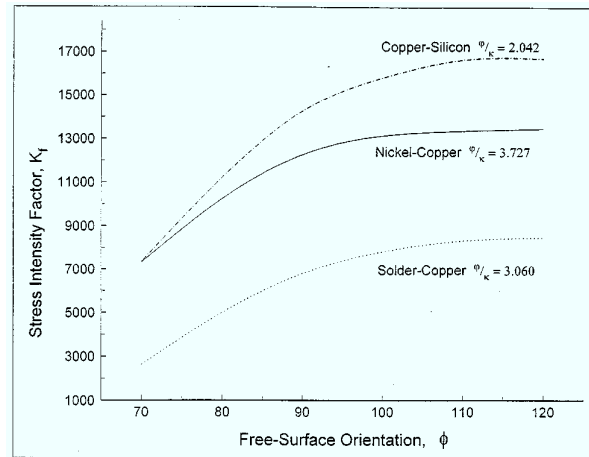


Figure 10. Free-edge stress intensity factor  $K_f$  vs. upper free surface orientation angle,  $\phi$  in copper-silicon, nickel-copper, and solder-copper bimaterials

imposing a displacement boundary condition across the upper surface of the specimen shown in Figure 1.

## 6. Summary

We have studied free-edge singularities and stress intensities in a variety of anisotropic bimaterials. The calculation for the order of the singularity was performed with the eigenvalue analysis of Ting (1996). The order of the singularity was shown to depend on the free-surface orientation as well as the elastic constants of the bimaterial. Free-surface orientation angles were determined below which the stress state was nonsingular. These critical angles were shown to be weakly dependent on the elastic constants for the bimaterial systems studied here. Free-edge stress-intensity factors were calculated with a local collocation method using the  $\sigma_{yy}$  component of stress along the interface. These stresses were determined from a boundary element analysis based on Green's functions for anisotropic bimaterials. It was noted that an assumption was made concerning the size of the singularity dominated zone for the data to be valid in the collocation for  $K_f$ . Singularity dominated zone sizes in fracture specimens were used as guidance for determining the region of validity of the free-edge asymptotic stress field. Future research will investigate this aspect of free-edge stress fields in more detail.

## Acknowledgments

The authors acknowledge the support of the National Science Foundation and the National Institute of Standards and Technology under the joint NSF-NIST program CMS-9522147 and for additional support provided by the NIST Center for Computational and Theoretical Materials Science, Dr. Sharon Glotzer, Director.

## References

- Bak, M. and Koenig, H.A. (1994). Prediction of edge stresses in layered media using the surface integral-finite element technique. *Engineering Fracture Mechanics* **48**, 583–593.
- Berger, J.R. (1994). Boundary element analysis of anisotropic bimetals with special Green's functions. *Engineering Analysis with Boundary Elements* **14**, 123–131.
- Bogy, D.B. (1972). The plane solution for anisotropic elastic wedges under normal and shear loading. *Journal of Applied Mechanics* **39**, 1103–1109.
- Cruse, T.A. (1988). *Boundary Element Analysis in Computational Fracture Mechanics*. Kluwer Academic Publishers, The Netherlands.
- Dundurs, J. (1969). Discussion of edge-bonded dissimilar orthotropic elastic wedges under normal and shear loading. *Journal of Applied Mechanics* **36**, 650–652.
- Ding, S. and Kumosa, M. (1994). Analysis of stress singular fields at a bimaterial wedge corner. *Engineering Fracture Mechanics* **49**, 569–573.
- Hein, V. L. and Erdogan, F. (1971). Stress singularities in a two-material wedge. *International Journal of Fracture* **7**, 317–330.
- Hirth, J.P. and Lothe, J. (1982). *Theory of Dislocations*, Second Edition. Krieger Publishing Co., Malabar, Florida.
- Mantic, V. and Paris, F. (1996). On Stroh orthogonality relations: an alternative proof applicable to Lekhnitskii and Eshelby theories of an anisotropic body. *Journal of Elasticity* **43**, 137–145.
- Reedy, E.D. (1990). Intensity of the stress singularity at the interface corner between a bonded elastic and a rigid layer. *Engineering Fracture Mechanics* **36**, 575–583.
- Sanford, R.J. and Chona, R. (1984). Photoelastic calibration of the short-bar chevron-notched specimen. *Chevron-Notched Specimens: Testing and Stress Analysis, ASTM STP 855* (Edited by J.H. Underwood, S.W. Freiman, and F.I. Baratta), American Society for Testing and Materials, Philadelphia, Pennsylvania, 81–97.
- Stroh, A.N. (1958). Dislocations and cracks in anisotropic elasticity. *Philosophical Magazine* **3**, 625–646.
- Tewary, V.K. (1991). Elastic Green's function for a bimaterial composite solid containing a free surface normal to the interface. *Journal of Materials Research* **6**, 2592–2608.
- Tewary, V.K. and Kriz, R.D. (1991). Generalized plane strain analysis of a bimaterial composite containing a free surface normal to the interface. *Journal of Materials Research* **6**, 2609–2622.
- Tewary, V.K., Wagoner, R.H. and Hirth, J.P. (1989). Elastic Green's function for a composite solid with a planar interface. *Journal of Materials Research* **4**, 113–123.
- Ting, T.C.T. (1995). Generalized Dundurs constants for anisotropic bimetals, *International Journal of Solids and Structures* **32**, 483–500.
- Ting, T.C.T. (1996). *Anisotropic Elasticity*. Oxford University Press.
- Zwiers, R.I., Ting, T.C.T. and Spilker, R.L. (1982). On the logarithmic singularity of free-edge stress in laminated composites under uniform extension. *Journal of Applied Mechanics* **49**, 561–569.